Biochemistry

 Volume 37, Number 10 March 10, 1998

Accelerated Publications

pH-Dependent Gating in the *Streptomyces lividans* K^+ Channel†

Luis G. Cuello,‡ Jesus G. Romero,‡ D. Marien Cortes,‡ and Eduardo Perozo*

Department of Molecular Physiology and Biological Physics and Center for Structural Biology, University of Virginia Health Sciences Center, Charlottesville, Virginia 22906-0011

Received December 5, 1997

ABSTRACT: Because of its size, high levels of expression, and unusual detergent stability, the small K^+ channel from *Streptomyces lividans* (SKC1) is considered to be an ideal candidate for detailed structural analysis. In this paper, we have used planar lipid bilayers and radiotracer uptake experiments to study purified and reconstituted SKC1, in an attempt to develop a bulk assay for its functional characterization. In channels reconstituted into liposomes with external pH 3.5 and intravesicular pH 7.5, a time-dependent SKC1-catalyzed $^{86}Rb^+$ uptake was observed. This cationic influx was blocked by Ba^{2+} ions with a K_i (external) of 0.4 mM and was shown to have the following selectivity sequence: $K^+ > Rb^+ > NH_4^+ \gg Na^+ > Li^+$. In experiments with external pH 7.5 or in liposomes containing no channels, no $^{86}Rb^+$ uptake was detected. When SKC1 was incorporated into planar lipid bilayers, we failed to observe significant single-channel activity at neutral pH but detected frequent multiple-channel openings a pH <5.0. These results indicate that under these experimental conditions SKC1 behaves as a pH-gated K^+ channel in which protonation of one or more residues promotes channel opening. At acidic pH and symmetrical 200 mM KCl solutions, SKC1 showed numerous brief openings with a main single-channel conductance of 135 pS and a subconductance state of 70 pS. Channel open probability showed a slight voltage dependence, with higher activities observed at negative potentials, a fact which may suggest that the protonation site lies within the transmembrane electrical field. Attempts to determine the pK_a of channel activation were obscured by intrinsic limitations of the $^{86}Rb^+$ flux assay. However, it appears to be lower than pH 4.0. Limited proteolysis experiments demonstrated that SKC1 reconstitutes vectorially, almost exclusively in the right-side-out configuration, indicating that the protonation site responsible for channel opening is located at the extracellular face of the channel. These results point toward a potentially novel gating mechanism for SKC1 and open the possibility of using transmembrane-driven radiotracer influx experiments as a reliable bulk functional assay for reconstituted SKC1.

Potassium channels are integral membrane proteins that catalyze K^+ ion flow across the membrane with exquisite selectivity and high efficiency. Their function has been associated with such basic cellular mechanisms as the regulation of electrical activity, signal transduction, and osmotic balance. Structurally, K^+ channels belong to the voltage-dependent cationic channel superfamily (*1*, *2*), which include Na^+ and Ca^{2+} channels as well as other K^+ channels not intrinsically voltage-dependent (i.e., the inward rectifier channels). These types of proteins conform to a common structural motif, involving multiple transmembrane (TM) segments arranged as helical bundles (*2*, *3*). These bundles

† This work was supported by USPHS Grant GM RO154690.

* Corresponding author: (e-mail) eperozo@virginia.edu; (phone) (804) 243-6580; (fax) (804) 982-1616.

‡ These authors contributed equally to this work.

S0006-2960(97)02997-8 CCC: $15.00
Published on Web 02/18/1998

form oligomeric structures by the association of subunits (as in K^+ channels) or homologous pseudosubunits (as in Na^+ and Ca^{2+} channels) around an ion-conductive pathway. Individual K^+ channel subunits are thought to be arranged in either two or six membrane-spanning segments, where the last two TM segments flank one (in some cases two) highly conserved loop known to play a key role in ion permeation and selectivity.

Despite the impressive body of information obtained from electrical measurements, it is clear that an understanding of ion channel function at the molecular level requires the high-resolution structure of an ion-selective channel. Some progress has been made recently with the solution structure of the inactivation particle of voltage-dependent K channels by NMR methods (*4*) and the impending structure of the *Shaker* tetramerization domain using X-ray crystallography (*5*). Still, the membrane-embedded segments of voltage-dependent channels continue to be refractory to traditional structural approaches. This is mainly due to their large size and intrinsic complexity and to the lack of a reliable biochemical preparation able to generate biochemical amounts of purified material.

The recent identification and cloning of a *Streptomyces lividans* K^+ channel (SKC1) (*6*) promises to offer a realistic alternative for high-resolution structural studies in K^+-selective channels. This channel (SKC1) is only 160 residues long and has two putative transmembrane segments and a well-defined "P region", reminiscent of that from other eukaryotic K channels (64% identity with Shaker's P loop). Additionally, SKC can be expressed in *Escherichia coli* at high levels and is easily purified by metal chelate chromatography (*6*−*8*). Initial biochemical characterization showed that SKC1 is tetrameric and extremely stable in detergent solution (*7*, *8*). Secondary structure analysis using circular dichroism spectroscopy revealed that SKC1 is mostly helical, with >55% α-helix and ∼30% β-structures (*7*), consistent with the notion that this class of proteins is arranged as a bundle of transmembrane helices.

An important requirement in the biochemical and structural characterization of ion channels is the establishment of a reliable functional assay capable of reporting on the whole population of molecules. Single-channel analysis can be used to describe channel gating and permeation properties with exquisite sensitivity and accuracy. Nonetheless, its use in characterizing purified channel preparations is limited by the very sensitivity that makes it so powerful for mechanistic studies (in theory, meaningful single-channel analysis could be obtained even when a fraction of the channels are functional). Therefore, successful characterization of purified channels requires both single-channel studies and bulk functional assays in the form of specific toxin binding or radiotracer flux measurements. However, although the functional analysis of purified SKC1 in planar lipid bilayers has shown that it behaves as a bona fide K^+ channel (*6*), efforts to generate functional evidence for a *population* of channels have, until now, unexpectedly failed (*7*, *8*). Among the possible explanations for these results have been to invoke special reconstitution conditions (lipid composition, detergent), lack of required auxiliary subunits, or intrinsic gating mechanisms. Thus, we have systematically searched for conditions in which a SKC1-catalyzed $^{86}Rb^+$ uptake could be detected as a way of developing a bulk assay for the functional characterization of SKC1.

In this report, we show that SKC1 behaves as a proton-activated K^+ channel, *increasing* its open probability as the extracellular pH *decreases*. Proton activation was demonstrated using vesicle $^{86}Rb^+$ uptake assays and single-channel analysis of SKC1 incorporated into lipid bilayers. In vesicles containing SKC1, the proton-induced permeability increase is K^+ selective and blocked by Ba^{2+} in the millimolar range. Although two main conductance states were detected in planar lipid bilayers (135 and 70 pS), the largest conductance state was by far, the most commonly observed. Analysis of SKC1 orientation in reconstituted vesicles indicated that the protonation site responsible for channel activation is located at the extracellular face of the channel, a result consistent with data from $^{86}Rb^+$ uptake and single-channel experiments. These results point toward a potential gating mechanism for SKC1 and allow transmembrane-driven radiotracer influx experiments to be used as a reliable bulk functional assay for reconstituted SKC1.

EXPERIMENTAL METHODS

Materials. Phospholipids were obtained from Avanti Polar Lipids (Birmingham, AL) Dowex 50-X8 was from Bio-Rad (Redmond, CA). $^{86}RbCl$ was purchased from Dupont (New England Nuclear). Talon Cobalt resin was from Clontech. TEMPONE (22,66-tetramethylpiperodine-*N*-oxyl) was purchased from Aldrich. Gramicidin D was a generous gift from Dr. Gabor Szabo (University of Virginia). All other reagents were of analytical grade.

SKC1 Purification and Reconstitution. Histidine-tagged SKC1 was expressed and purified after sequential metal chelate chromatography in a cobalt resin (Talon, Clontech) and gel filtration chromatography on a Superdex 200 column as previously described (*7*). Purified SKC1 in 200 mM dodecyl maltoside and a K^+-containing buffer (90−170 mM KCl, 20 mM Tris buffer pH 7.6) was reconstituted into preformed asolectin liposomes at lipid-to-protein ratios up to 20000:1 (molar) by the dilution method (*7*), centrifuged at 100000*g*, and resuspended in the same buffer at 1 mg/mL final protein concentration. This procedure was repeated twice before proceeding with the functional assays.

$^{86}Rb^+$ Flux Assays. K^+ channel activity was measured following the method of Garty et al. (*9*), with some modifications. For each assay, 50−100 μg of reconstituted channel was used (in 100-μL aliquots). A large K^+ gradient was established just before the start of the experiment by exchanging external K^+ for choline through gel filtration chromatography in Sephadex G-25 (1.5 mL final pooled volume). In those vesicles containing open K^+ channels, a large diffusion potential, negative inside develops. This transmembrane potential drives the accumulation of external Rb^+ into the vesicles.

Dowex 50-X8 was changed into the Tris form by equilibration in 1 M Tris-HCl buffer pH 7.0. This was followed by washing with several volumes of cold isosmolar sucrose. Each assay was initiated by the addition of 20 nmol of $^{86}RbCl$ (∼4.7×10^6 cpm) to the vesicle suspension. The ^{86}Rb uptake was stopped by quickly loading a 100-μL aliquot into a 1-mL Dowex column, and the vesicles were eluted directly into scintillation vials with 1.5 mL of isosmolar

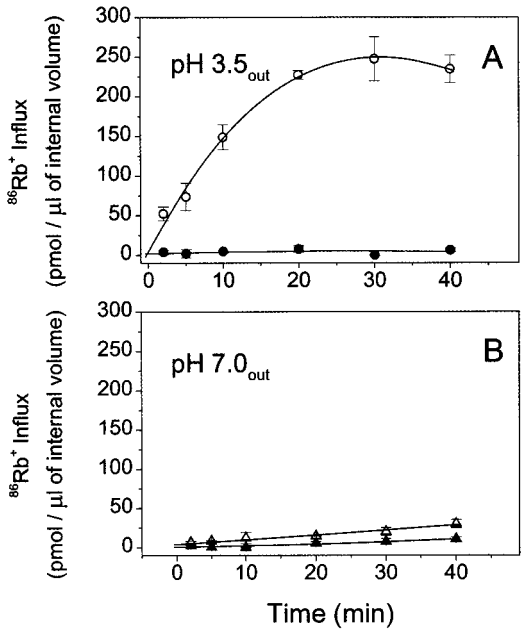

FIGURE 1: Time course of $^{86}Rb^+$ uptake dependency on extravesicular pH. (A) Open circles, uptake at pH 3.5; filled circles, uptake at pH 3.5 in the presence of 10 mM $BaCl_2$ in both sides of the membrane. (B) Open triangles, uptake at pH 7.0; filled circles, uptake at pH 7.0 in the presence of 10 mM $BaCl_2$ in both sides of the membrane. Data are shown as mean ± standard deviation ($n = 3$). The smooth curves are drawn by eye.

sucrose, 20 mM PBS pH 7.6. Trapped $^{86}Rb^+$ was quantified by scintillation counting.

Planar Lipid Bilayer Measurements. Planar lipid bilayers were made according to the method of Muller et al. (*10*). Bilayers were formed from a solution of 20 mg/mL phospholipid in decane using either acetone/ether-purified asolectin lipids (*11*) or a mixture of 1,2-dioleoyl-glycero-3-phosphatidylethanolamine and 1,2-dioleoyl-glycero-3-phosphatidylserine (9:1). The lipid solution was painted on a 400-μm hole in a Teflon partition separating two 1-mL compartments (cis and trans). These were electrically connected to the recording system through Ag/AgCl electrodes and agar bridges filled with 1 M KCl. The trans side was referred to ground while the cis side was connected to the bilayer amplifier. The current across the bilayer was measured with a homemade low-noise current-to-voltage converter, filtered at 1 kHz with a eight-pole low-pass Bessel filter, digitized, and stored on video tapes for later analysis. Bilayer formation was followed both optically and electrically. Unless otherwise noted, single-channel recordings were made on symmetrical KCl buffer solutions (200 mM KCl, 5 mM of the appropriate buffer). After bilayer formation, proteoliposomes containing the reconstituted SKC1 were added to the trans side under constant stirring to promote liposome fusion. Single-channel analysis was performed with TRANSIT (*12*) and Origin (Northamptom MA) software packages.

Quantification of Liposome Internal Volume. The internal volume of SKC1-containing vesicles was obtained using the spin-label broadening method according to Vistnes and Puskin (*13*). We used the membrane permeant spin label TEMPONE and chromium oxalate as a broadening agent. Internal volume was expressed as the fraction of total volume and was used to normalize the magnitude of the $^{86}Rb^+$ uptake.

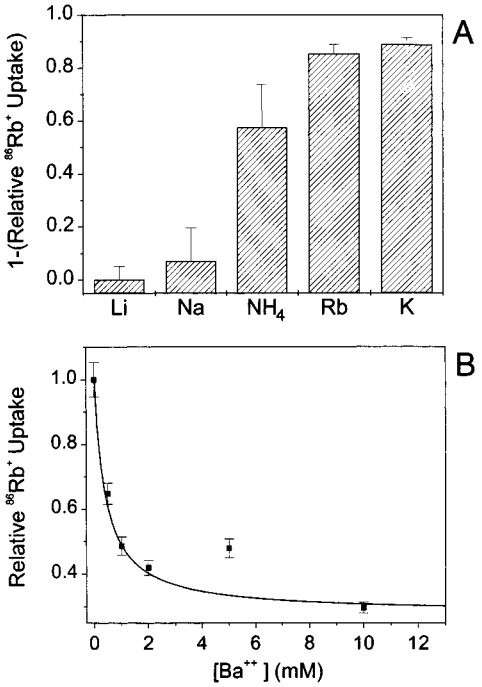

FIGURE 2: SKC1 ion selectivity and Ba^{2+} block. (A) Values for the $^{86}Rb^+$ uptake at 60 min were obtained after exchanging extravesicular K^+ for a number of permeant cations. Data are presented as 1 − (relative $^{86}Rb^+$ uptake) to display relative ion permeation. (B) $^{86}Rb^+$ uptake was measured after a 5-min incubation with a given Ba^{2+} concentration in the extravesicular solution. Ba^{2+} was added after the establishment of a transmembrane potential against LiCl. The smooth curve was drawn according to the equation $Y = (1 + [Ba^{2+}]/K_i)^{-1}$, with $K_i = 0.4$ mM.

Determination of SKC1 Vectoriality. SKC1 (10 μg), reconstituted by the dilution method into asolectin liposomes, was incubated for 2 h at room temperature with 5 μg/mL trypsin. The reaction was stopped by addition of protease inhibitors (PMSF, 0.7 mg/mL and leupeptin, 25 μg/mL) and the sample run on 15% gels. For comparison, an identical amount of channel, solubilized in 200 μM dodecyl maltoside, was subjected to the same treatment and run on the same gel. The relative amounts of inside-out versus outside-out channels can be calculated from the integrals of the individual bands obtained after digitizing Comassie-stained gels.

RESULTS AND DISCUSSION

Proton-Activated $^{86}Rb^+$ Fluxes in Reconstituted SKC1. The physiology of prokaryotic organisms is based on the establishment and maintenance of a proton electrochemical gradient ($\Delta\mu H^+$) across the plasma membrane (*14*, *15*). In Gram-positive bacteria (such as *Streptomyces*), the cell membrane is surrounded by a thick peptidoglycan layer (*16*) which contributes to generate a large unstirred layer. We thus reasoned that since intracellular pH is normally regulated around neutral values, the immediate extracellular environment of SKC1 is most likely acidic and that protons could play a role in opening and closing the channel. Proton levels can have dramatic effects on channel properties, from open-channel blocking to direct effects on channel gating properties (*17*). In general, ion channels tend to be fairly insensitive to external proton concentration but are inhibited by lowering intracellular pH, as in the case of a number of inward rectifier channels (*18*−*20*). Thus we chose to change external pH for the initial flux experiments. Our experimental strategy

to measure radiotracer accumulation into channel-containing liposomes is based on the method of Garty et al. (*9*). In this approach, the extent of $^{86}Rb^+$ accumulation is directly proportional to both the open channel probability and its ability to generate a transmembrane potential in the presence of a K^+ gradient. Notice that if the reconstituted channels are nonselective, or reside in the closed configuration, no transmembrane potential can be generated and thus no radiotracer accumulation occurs.

$^{86}Rb^+$ uptake experiments were carried out in vesicles containing 90 mM KCl buffered at pH 7.6 with PBS inside, while the external solution was exchanged for isosmolar choline chloride buffered at a chosen pH using citrate or HEPES buffers. Figure 1 shows the result of an experiment in which SKC1, reconstituted at a lipid-to-protein ratio of 5000:1 (molar) was incubated at either acidic or neutral external pH prior to the initiation of the assay. In the presence of extravesicular pH 3.5, we detected a large, time-dependent increase in $^{86}Rb^+$ permeability (Figure 1A, open circles), which was nearly abolished by the presence of 10 mM Ba^{2+} in both sides of the membrane (filled circles). If the vesicles are incubated at external pH 7.6 (Figure 1B, open triangles), the $^{86}Rb^+$ uptake is sharply reduced, and that influx is still inhibited by Ba^{2+}. Experiments in which the pH gradient was reversed (pH 3.5 inside and 7.6 outside) failed to show Ba^{2+}-sensitive $^{86}Rb^+$ accumulation at any pH (not shown), suggesting that these channels reconstitute mostly in a preferred orientation.

The importance of these results cannot be overstated, since they allow for the functional characterization of a whole population of SKC1 channels under various conditions. They also indicate that purified and reconstituted SKC1 is at least selective against chloride, the only other likely permeant ion present in the assay. Further characterization of SKC1 cationic selectivity and its blockage by external Ba^{2+} ions was performed by comparing the relative extent of the $^{86}Rb^+$ uptake under different biionic conditions. Figure 2A shows the relative permeability of a number of monovalent cations through SKC1. In this experiment, external choline was substituted for a number of test cations and the $^{86}Rb^+$ uptake assayed at pH 4.0. As the accumulation of $^{86}Rb^+$ depends on the magnitude of the transmembrane potential generated at each biionic condition, the lower the permeability of the external cation, the larger the $^{86}Rb^+$ uptake. Therefore, to present the data in terms of relative permeabilities, we have plotted 1 − (relative uptake) for each of the test cations. From the data in Figure 2A, the selectivity series for SKC1 was found to be $K^+ > Rb^+ > NH_4^+ \gg Na^+ > Li^+$, which is identical to the selectivity series of a number of different K^+ channels (see ref *17*). Figure 2B illustrates the effect of various external Ba^{2+} concentrations upon $^{86}Rb^+$ uptake. There is a clear reduction in the amount of captured $^{86}Rb^+$ after 30 min of incubation, and the inhibition reaches up to 70% of the total uptake. When Ba^{2+} was present in both sides of the membrane, the inhibition of the $^{86}Rb^+$ uptake was less than 10% of the control value (not shown). The continuous curve shows the fit to the data using a binding isoterm with a single K_i of 0.4 mM.

Single-Channel Properties in Planar Lipid Bilayers. Independent experiments were performed in planar lipid bilayers to characterize SKC1 single-channel behavior at low pH. Recordings were obtained in symmetrical 200 mM KCl with 5 mM citrate buffer pH 4.0. Vesicles used for channel incorporation contained SKC1 reconstituted at a 20000:1 lipid-to-protein ratio (molar). Figure 3A shows representative single-channel traces obtained at a range of potentials. From these recordings, a single-channel $I-V$ relation was obtained for two conductance states (Figure 3A, bottom panel), a large 135-pS opening displaying brief openings, and a 70-pS opening with longer open times, the largest one being by far the most populated state. Rarely, an additional subconductance level of 30 pS was also observed. When these experiments were repeated at pH 7.0, no single-channel activity was present, even after repeated attempts. However, in experiments with asymmetric pH levels (pHs 4.0 and 7.0), single-channel activity was observed only when the acidic pH was applied to the trans side of the bilayer, also suggesting that SKC1 incorporates into the bilayer with a preferred orientation. Previous analysis of SKC1 single-channel currents by Schrempf et al. (*6*) also revealed a multiconductance behavior with single-channel conductances around 20, 40, and 90 pS under nonsymmetric conditions. In contranst to our present observations, analysis of purified and reconstituted SKC1 in planar bilayer indicated that the 40-pS subconductance was most frequently observed. However, as these studies were performed at neutral pH, there is a distinct possibility that proton binding may be shifting the relative occupancy of the individual subconductance states toward the larger conductance.

The open probability of SKC1 showed considerable voltage dependence, with higher single-channel activity at negative potentials. This point is illustrated in Figure 3B, where the activity from a multichannel bilayer in symmetrical pH 4.0 solutions was sequentially recorded at +60 and −60 mV. At 60 mV, SKC1 opens with numerous brief apertures and shows a low frequency of multiple simultaneous openings, as expected given its low open probability. Comparatively, at −60 mV there is a noticeable increase in the open probability and in the number of multiple openings (up to four). Also, from the corresponding amplitude histograms, it appears that the relative occupancy of the 70-pS subconductance state increases at positive potentials. It is unlikely that this voltage-dependent behavior is the result of an intrinsic voltage gating process, particularly in view of the fact that there appear to be no charged residues within the two putative transmembrane segments (*6*). However, if the gating process depended on the protonation of a site located within the transmembrane electrical field, a voltage-dependent behavior would be expected due to changes in the local proton concentration, particularly at extreme voltages. In fact, placing this site toward the extracellular face of the channel would render voltage dependencies consistent with the observed experimental behavior (higher open probability at negative potentials). A detailed analysis of this phenomenon is being currently pursued in our laboratory.

Under present experimental conditions, each single-channel opening is brief (<0.5 ms) and the absolute open probabilities are small. Therefore, a detailed analysis of this effects has not been carried out due to uncertainties in the determination of the number of channels. However, an indication of the open probabilities at these two potentials can be obtained from the relative areas of the conducting and nonconducting peaks of the amplitude histograms. These values are proportional to the open probability weighted to

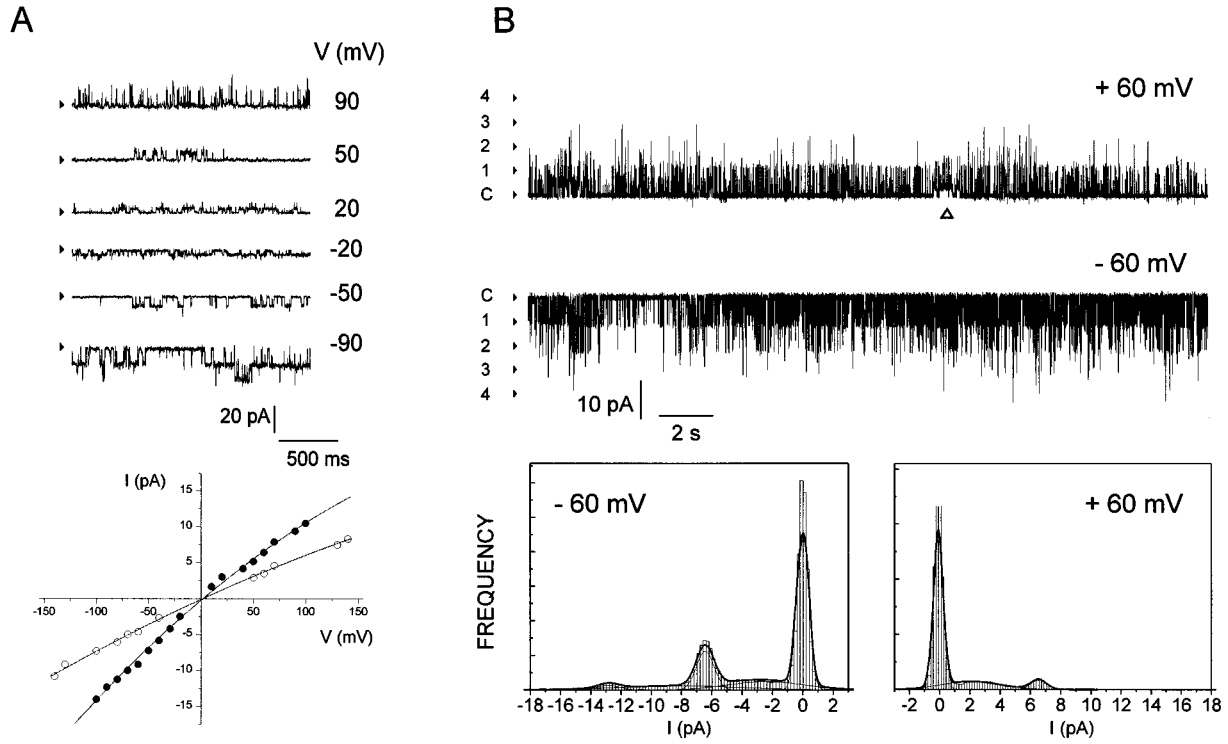

FIGURE 3: Single-channel traces of SKC1 incorporated into planar lipid bilayers. (A) Traces obtained at a wide voltage range were used to generate an $I-V$ plot (lower panel). Two conductance states were observed with single-channel conductances of 140 and 70 pS. (B) Apparent voltage dependence of SKC1 activation. Single-channel traces were recorded at +60 (top trace) or −60 mV (lower traces) under symmetrical conditions in a solution containing 200 mM KCl and 20 mM citrate buffer pH 4.0. Each of the multiple opening levels corresponding to the largest conductance value of SKC1 is labeled with a number. An open arrow tip points to a subconductance opening. The closed state corresponds to level C. The lower two panels represent the all point histograms calculated from the above traces. Data were fitted with a sum of Gaussian peaks defined by a midpoint (χ, in pA) and a standard deviation (σ, in pA). Parameters for the data at −60 mV: $\chi_1 = 0$, $\sigma_1 = 0.58$, $\chi_2 = -2.45$, $\sigma_2 = 5.07$, $\chi_3 = -6.44$, $\sigma_3 = 1.04$, $\chi_4 = -8.07$, $\sigma_4 = 8.12$, $\chi_5 = -12.83$, and $\sigma_5 = 1.34$. Parameters for the data at 60 mV: $\chi_1 = -0.02$, $\sigma_1 = 0.48$, $\chi_2 = 2.71$, $\sigma_2 = 3.89$, $\chi_3 = 6.53$, and $\sigma_3 = 0.98$.

the number of channels (NP_o) and have been calculated to be $NP_o = 0.29$ at 60 mV and $NP_o = 0.51$ at −60 mV, a 75% increase at the negative potential. This voltage effect on open probability can also be seen from the current traces in Figure 3A, particularly at +90 and −90 mV.

pH Dependence of SKC1 activity. Proton-gated channels have been described in a number of preparations, including plant guard cells (*21*), toad epithelial cells (*22*), and sensory neurons (*23*), and their pH-dependent gating properties are generally compatible with single-protonation reactions with pK_a for activation usually at pH ∼6. Figure 4 shows the pH dependence of SKC1 activation, studied from uptake experiments and from single-channel measurements in planar lipid bilayers. Using the same type of experiment as in Figure 1, the maximum value of the $^{86}Rb^+$ uptake has been plotted against a series of pHs ranging from pH 2.0 to 7.0 (Figure 4A). The $^{86}Rb^+$ uptake tends to increase as the pH is lowered from neutral values, reaches a maximum around pH 4.0, and then decreases sharply at lower pH values. This type of behavior is not unusual in proteins (see ref *24*) and would indicate that two protonation−deprotonation reactions may be involved in the pH-dependent gating of SKC1. We have analyzed these results according to a two-independent-site model described by:

$$\text{cpm} = \left(\frac{1}{1 + e^{(-(\text{pH} - \text{p}K_{a1}))/\alpha}}\right) * \left(\text{cpm}_0 + \frac{\text{cpm}_{max}}{1 + e^{(\text{pH} - \text{p}K_{a2})/\beta}}\right) \quad (1)$$

where cpm_0 is the basal $^{86}Rb^+$ uptake at neutral pH, cpm_{max} is the maximum $^{86}Rb^+$ uptake, and α and β are the slope constants of two independent protonation reactions with pK_{a1} and pK_{a2}. There are two physical interpretations to this pH dependence model. One possibility is that SKC1 is opened by the protonation of one specific residue and closed by the additional protonation of a second residue with a lower pK_a. This is the standard interpretation for the pH effects on enzyme activity. The second possibility is that SKC1 is opened by a simple one-site protonation reaction, but this process is partially masked by a pH effect on the basal vesicle permeability that reduces the transmembrane potential. Given the absolute dependence of $^{86}Rb^+$ uptake on the direction and magnitude of the transmembrane potential generated during the assay, this effect would be highly inhibitory.

The data from Figure 4A was fitted with eq 1 and plotted as continuous line using the following values: $pK_{a1} = 3.56$, $\alpha = 0.22$, $pK_{a2} = 2.64$, $\beta = 0.7$, $\text{cpm}_0 = 500$, $\text{cpm}_{max} = 26\,755$. Two points are worth noting about these values. First, the pK_a value for the inhibitory process (pK_{a1}) is *larger* than that for the protonation reaction that activates the channel (pK_{a2}). Second, the value of cpm_{max} is severalfold greater than the largest uptake observed experimentally (at pH 4.0), implying that we detect only a fraction of the total uptake capacity of the system at lower pHs. Together, these results suggest that the reduction in the values for $^{86}Rb^+$ uptake at pHs lower than 4.0 is the result of a measurement

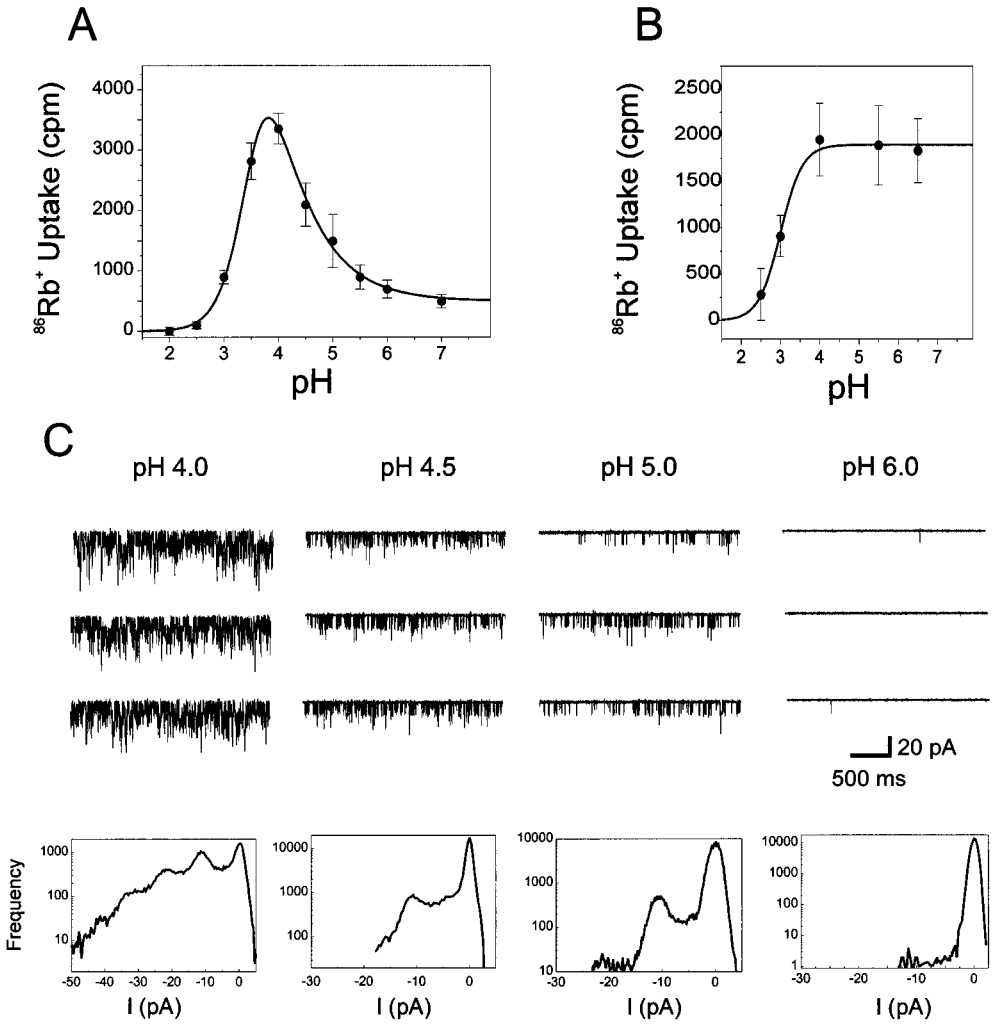

FIGURE 4: pH dependence of SKC1 activation. (A) Data from $^{86}Rb^+$ uptake experiments where the extravesicular pH was changed at the moment the K^+ difussion potential was established. Uptake values after 30 min are reported. All experiments were performed with Na^+ as the external ion. Data are reported as mean ± standard deviation ($n = 4$). The continuous line is drawn according to eq 1 with the following parameters: $pK_{a1} = 3.56$, $\alpha = 0.22$, $pK_{a2} = 2.64$, $\beta = 0.7$, $cpm_0 = 500$, and $cpm_{max} = 26\,755$. (B) Identical experiment as in (A) but using reconstituted gramicidin D (2×10^{-5} M) and choline as the external ion. The smooth line was drawn according to the equation $Y = cpm_{max}/(1 + \exp(pK_a - pH)/\alpha)$, with $pK_a = 3.1$, $cpm_{max} = 1654$, and $\alpha = 0.28$. (C) pH effect on single-channel properties of SKC1. Top: consecutive single-channel traces obtained at pH 4.0, 4.5, 5.0, and 6.0 for a multichannel asolectin bilayer. Bottom panels: All point histogram corresponding to each set of single-channel records. Data were fitted with multiple Gaussians and their relative areas used to compute the NP_o values for each pH: $NP_o = 0.73$ (pH 4.0), $NP_o = 0.42$ (pH4.5), $NP_o = 0.11$ (pH 5.0), and $NP_o = 5 \times 10^{-4}$ (pH 6.0).

artifact, probably originated by an increase in the nonspecific permeability of the vesicles at low pH.

This possibility was directly addressed by the experiment in Figure 4B. Here, we have performed an identical pH dependence experiment using gramicidin, a channel in which the open probability is not reduced at low pH (*25*). Gramicidin is also known to have a high proton permeability, which will tend to affect the K^+-generated diffusion potential, particularly at low pH values. Clearly, these data shows a sharp inhibition in the magnitude of $^{86}Rb^+$ uptake at lower pHs, a fact that supports the notion that the reduction in the $^{86}Rb^+$ uptake in the SKC1 experiments may be a consequence of a measuring artifact. The data in Figure 4B were fitted with a single protonation site model with $pK_a = 3.1$ and $\alpha = 0.28$, values that are remarkably similar to those obtained from the fit to the data in Figure 4A.

Given the inability of the present uptake assay to report accurately on fluxes at lower pHs, the actual value of the p*K* for the proton activation of SKC1 cannot be determined with certainty. However, it is clear that this value is well below the experimentally obtained optimum of pH 4.0, and it is probably close to pH 2.6, as determined from the fit of eq 1 to the data. This value is lower than the pK_as for the protonation of free acidic amino acids (Asp, $pK_a = 3.9$; Glu, $pK_a = 4.3$) suggesting that this particular protonation site might be interacting with neighboring groups. Such pK_a shifts toward acidic values would be compatible with the presence of a salt bridge (*26*). This type of interaction has been recently confirmed in the inward rectifier channel family of channels (*27*).

Figure 4C shows the single-channel behavior of SKC1 recorded at different pH values. These recordings were obtained by holding the bilayer at −100 mV in symmetrical 200 mM K_2SO_4 with 20 mM citrate buffer (pHs 4.0, 4.5, and 5.0) or MES buffer (pH 6.0). We found a large increase in SKC1 single-channel activity as the pH of the solution decreased but detected no apparent changes in its single-channel conductance. Attempts to obtain reliable measurements at pHs lower than 3.5 were unsuccessful due to low bilayer stability. The weighted open probability (NP_o),

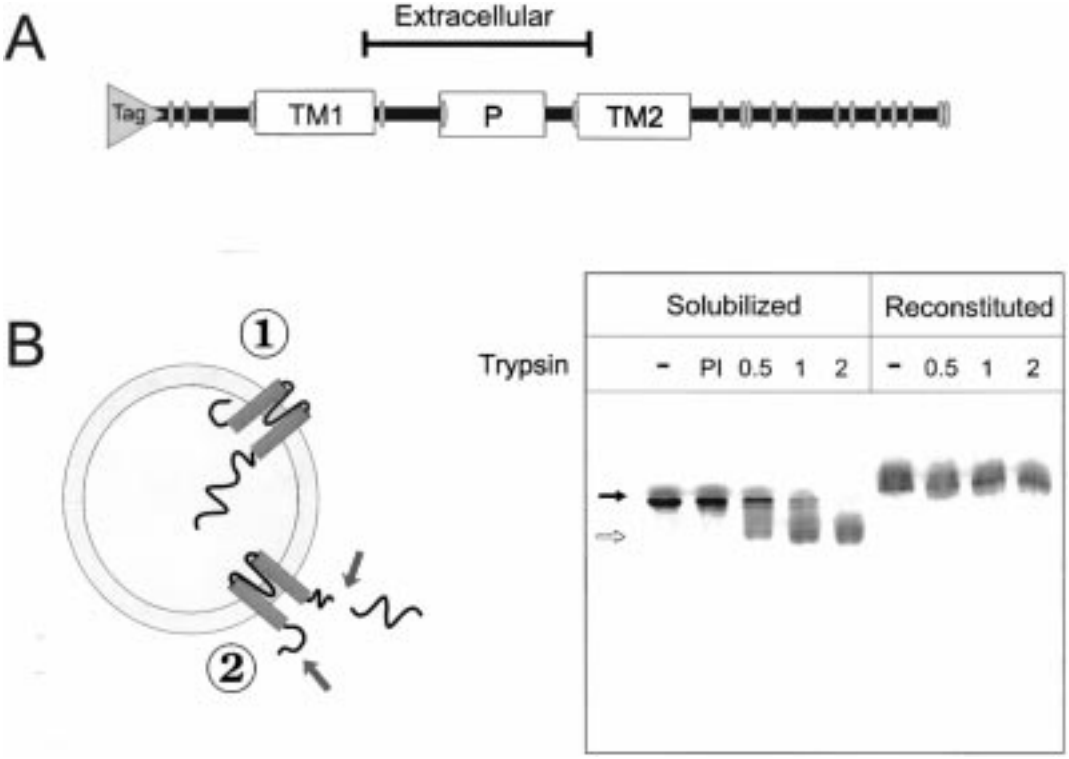

FIGURE 5: Determination of SKC1 vectorial reconstitution from limited proteolysis experiments. (A) Predicted topology of SKC1 with the location of potential trypsin cleavage sites (ovals). (B) Left panel: the two possible orientations of reconstituted SKC1 and their relative susceptibilities to proteolysis. Right panel: time course of trypsin proteolysis for solubilized and reconstituted SKC1. Shown are control conditions in the absence of trypsin (−), with trypsin and protease inhibitors (PI) and at 0.5-, 1-, and 2-h incubations at room temperature. The filled arrow points to the intact channel (~64 kDa); the open arrow to the main cleavage product (~45 kDa).

calculated from the relative areas of the conductive and nonconductive peaks of the amplitude histogram were $NP_o = 0.73$ at pH 4.0, $NP_o = 0.42$ at pH 4.5, $NP_o = 0.11$ at pH 5.0, and $NP_o = 5 \times 10^{-4}$ at pH 6.0; a ~1500-fold factor from pH 6.0 to pH 4.0. The general tendency of these NP_o values argues that the pK_a for SKC1 activation may be lower than 4.0, in agreement with the conclusions derived from the $^{86}Rb^+$ uptake experiments.

Vectoriality of Reconstituted SKC1. Results from $^{86}Rb^+$ uptake and planar lipid bilayer experiments have suggested that SKC1 must reconstitute vectorially to account for the data. We have further analyzed the apparent sideness of the reconstitution of SKC1 by performing limited proteolysis experiments on solubilized and reconstituted SKC1. Figure 5A shows the location of potential trypsin sites in relation to a one-dimensional topological model of SKC1 based on hydrophobicity analysis (*7*). In this model, both terminal segments of SKC1 are located intracellularly, while the P loop and limited portions of the two transmembrane segments are exposed to the extracellular space. Clearly, the majority of potential trypsin cleavage sites are located at the N- and C-termini of the channel. This asymmetric susceptibility to trypsin cleavage allows us to distinguish between inside-out and right-side-out reconstituted channels, so that the trypsin proteolytic pattern of reconstituted SKC1 can be used to quantify the relative orientation of the channel in the bilayer (Figure 5B). Figure 5C shows the results of a trypsin proteolysis experiment on solubilized and reconstituted SKC1. In detergent solution, a 2-h incubation of SKC1 with trypsin at room temperature reduces the apparent size of the tetrameric complex (64 kDa) and generates a number of bands around 45 kDa. The size of the cleaved product clearly indicates that trypsin is cutting the solubilized channel near the C- and N-termini. The fact that we were able to purify the trypsinized tetramer after incubation with 20 μL of cobalt-containing resin (not show) establishes the location of the cleavage sites at the C-terminus. The same amount of reconstituted SKC1 remains intact after 2 h of incubation with trypsin. Under these conditions, SKC1 tetramer bands run slightly higher and broader, probably due to the presence of lipid in the sample. These results indicated that when SKC1 is incorporated into asolectin vesicles from a DDM solution, it reconstitutes almost exclusively in the outside-out configuration (configuration 1 in Figure 5B). This finding is in agreement with the results of the $^{86}Rb^+$ uptake and the bilayer incorporation experiments and implies that the protonation reaction responsible for SKC1 activation occurs at the extracellular face of the channel.

CONCLUSIONS

The present results show very convincingly that the gating mechanism of purified and reconstituted SKC1 is regulated by the proton concentration in the extracellular face of the channel. This regulation occurs in the form of a proton-dependent increase in open probability without changes in open channel behavior. Although it is quite possible that this protonation effect may not be the SKC1 primary gating mechanism, it might still play an important modulator role. More importantly, these findings have opened the possibility of using bulk assays, like radiotracer influx measurements, to probe the functional behavior of purified SKC1 under a wide range of conditions and to quickly assess the general effects of site-directed mutants generated for site-directed spin-labeling and other reporter group approaches. This type

of assay will prove very useful for future biochemical characterization of SKC1.

ACKNOWLEDGMENT

We thank Dr. Gabor Szabo for numerous insightful discussions and unrestricted access to his bilayer setup. Dr Szabo also provided useful comments on the manuscript.

REFERENCES

1. Catterall, W. A. (1995) *Annu. Rev. Biochem. 64*, 493−531.
2. Jan, L. Y., and Jan, Y. N. (1997) *Annu. Rev. Neurosci. 20*, 91−123.
3. Miller, C. (1991) *Science 252*, 1092−6.
4. Antz, C., Geyer, M., Fakler, B., Schott, M. K., Guy, H. R., Frank, R., Ruppersberg, J. P., and Kalbitzer, H. R. (1997) *Nature 385*, 272−5.
5. Kreusch, A., Pfaffinger, P. J., Stevens, C. F., and Choe, S. (1996) in *XVII Congress of the International Union of Crystallography*, Seattle, WA, pp C-169.
6. Schrempf, H., Schmidt, O., Kummerlen, R., Hinnah, S., Muller, D., Betzler, M., Steinkamp, T., and Wagner, R. (1995) *EMBO J. 14*, 5170−8.
7. Cortes, D. M., and Perozo, E. (1997) *Biochemistry 36*, 10343−52.
8. Heginbotham, L., Odessey, E., and Miller, C. (1997) *Biochemistry 36*, 10335−42.
9. Garty, H., Rudy, B., and Karlish, S. J. (1983) *J. Biol. Chem. 258*, 13094−9.
10. Mueller, P., Rudin, D. O., Tien, H., and Wescott, W. C. (1962) *Nature 194*, 979−80.
11. Kagawa, Y., Kandrach, A., and Racker, E. (1973) *J. Biol. Chem. 248*, 676−84.
12. VanDongen, A. M. (1996) *Biophys. J. 70*, 1303−15.
13. Vistnes, A. I., and Puskin, J. S. (1981) *Biochim. Biophys. Acta 644*, 244−50.
14. Haddock, B. A. (1980) *Philos. Trans. R. S. London Ser. B: Biol. Sci. 290*, 329−39.
15. Skulachev, V. P. (1991) *Biosci. Rep. 11*, 387−441 (discussion 441−4).
16. Reusch, V. M., Jr. (1984) *Crit. Rev. Microbiol. 11*, 129−55.
17. Hille, B. (1992) *Ion channels of excitable membranes*, 2nd ed., Sinauer, Sunderland, MA.
18. Blatz, A. L. (1984) *Pflugers Arch.−Eur. J. Physiol. 401*, 402−7.
19. Fakler, B., Schultz, J. H., Yang, J., Schulte, U., Brandle, U., Zenner, H. P., Jan, L. Y., and Ruppersberg, J. P. (1996) *EMBO J. 15*, 4093−9.
20. Sabirov, R. Z., Okada, Y., and Oiki, S. (1997) *Pflugers Arch.−Eur. J. Phys. 433*, 428−34.
21. Blatt, M. R. (1992) *J. Gen. Physiol. 99*, 615−44.
22. Lacaz-Vieira, F. (1995) *J. Membr. Biol. 148*, 1−11.
23. Waldmann, R., Champigny, G., Bassilana, F., Heurteaux, C., and Lazdunski, M. (1997) *Nature 386*, 173−177.
24. Fersht, A. R. (1985) *Enzyme structure and mechanism*, 2nd ed., Freeman, New York.
25. Myers, V. B., and Haydon, D. A. (1972) *Biochim. Biophys. Acta 274*, 313−22.
26. Nakamura, H. (1996) *Q. Rev. Biophys. 29*, 1−90.
27. Yang, J., Yu, M., Jan, Y. N., and Jan, L. Y. (1997) *Proc. Natl. Acad. Sci. U.S.A. 94*, 1568−72.

BI972997X